

# Nonequilibrium steady state for strongly-correlated many-body systems: variational cluster approach

Michael Knap,\* Enrico Arrigoni, and Wolfgang von der Linden

*Institute of Theoretical and Computational Physics,  
Graz University of Technology, 8010 Graz, Austria*

(Dated: March 29, 2019)

A numerical approach is presented that allows to compute non-equilibrium steady state properties of strongly correlated quantum many-body systems. The method is imbedded in the Keldysh Green's function formalism and is based upon the idea of the variational cluster approach as far as the treatment of strong correlations is concerned. It appears that the variational aspect is crucial as it allows for a self-consistent adjustment of the equilibrium reference system to the nonequilibrium target state. The approach is neither perturbative in the many-body interaction nor in the field, that drives the system out of equilibrium, and it allows to study strong perturbations and nonlinear responses of systems in which also the correlated region is spatially extended. We apply the presented approach to non-linear transport across a strongly correlated quantum wire described by the fermionic Hubbard model.

PACS numbers: 71.27.+a 47.70.Nd 73.40-c 05.60.Gg 68.65.La

## I. INTRODUCTION

The theoretical understanding of the nonequilibrium behavior of strongly correlated quantum many-body systems is a long standing challenge, which has become increasingly relevant with the progress made in the fields of quantum optics and quantum simulation, semiconductor, quantum, and magnetic heterostructures, nanotechnology, or spintronics. In the field of quantum optics and quantum simulation recent advances in experiments with ultracold gases in optical lattices shed new light on strongly-correlated many body systems and their nonequilibrium properties. In these experiments, specific lattice Hamiltonians can be engineered and studied with a remarkable high level of control, making strong correlations observable on a macroscopic scale.<sup>1-3</sup> In this field another very promising experimental setup to study correlation effects are coupled cavity quantum electrodynamic systems which contain some form of optical nonlinearity resulting from the interaction of light with atomic levels.<sup>4,5</sup> These coupled cavity systems are inherently out of equilibrium, since they are driven by external lasers and susceptible to dissipation. Semiconductor, quantum, and magnetic heterostructures subject to a bias voltage also display nonequilibrium physics, where strong correlations play a decisive role. Experiments which study transport in molecular junctions demonstrate that many-body effects, also in combination with vibrational modes are crucial, see, e.g., Refs. 6,7. Another class of material structures with remarkable nonequilibrium properties are (multi-well) heterostructures of diluted magnetic semiconductors (DMSs) and superlattices embedded in normal metals. These systems are of great interest as they open the possibility to tailor electronic and spintronic devices for computing and communications based on their unique interplay of spin and electronic degrees of freedom. Moreover, they display a pronounced non-linear transport behavior.<sup>8-14</sup> The source of nonlinearity

is also related to the strong interaction between charge carriers, excitations and vibrational modes. In addition, spin degrees of freedom clearly play a major role in their transport properties. In order to fabricate technologically useful structures the theoretical understanding of these highly correlated quantum many-body systems is indispensable.

The typical nonequilibrium situation in all these systems is described by switching on a perturbation at a certain time  $\tau = \tau_0$ , for example, a bias voltage, which is kept constant beyond a time  $\tau'_0$ , specifying that the switching process itself has finished. For this problem one may, on the one hand be interested in transient properties at short times after switching on the perturbation, for example in ultrafast pump-probe spectroscopy.<sup>15</sup> In this case, the properties of the system depend on the initial state, as well as on the line shape of the switch-on pulse between  $\tau_0$  and  $\tau'_0$ . For longer times away from  $\tau_0$ , quite generally one expects the system to reach a steady state, whose properties do not depend on details of the initial state. Nonequilibrium steady states are relevant, for example, in quantum electronic transport across heterostructures, quantum dots, molecules (see, e.g., Refs. 16-21) or in driven-dissipative ultracold atomic systems.<sup>22-27</sup> Among the methods to treat strongly correlated systems out of equilibrium, one should mention density-matrix renormalization group and related matrix-product state methods,<sup>28-32</sup> continuum-time quantum Monte-Carlo,<sup>33</sup> functional renormalization group,<sup>34</sup> equation-of-motion methods,<sup>18,21</sup> numerical renormalization group,<sup>35</sup> dynamical mean-field theory,<sup>36-38</sup> scattering Bethe Ansatz,<sup>39</sup> and the dual-fermion approach.<sup>40</sup> Recently, Balzer and Potthoff<sup>41</sup> have presented a generalization of cluster-perturbation theory (CPT) to the Keldysh contour, which allows for the treatment of time-dependent phenomena. Their results show that CPT describes quite accurately the short and medium-time dynamics of a Hubbard chain.

Here, we propose a variational cluster method, which allows to study steady-state properties of strongly correlated many-body systems. When studying a nonequilibrium steady state of an isolated quantum many-body system, it is essential for the system volume  $\mathcal{V}$  to be truly infinite, in order to provide a relaxation mechanism. In this respect, the order of the limits ( $\mathcal{V} \rightarrow \infty$  before  $\tau_0 \rightarrow -\infty$ ) is essential (see, e.g. Ref. 42 for a discussion).

The paper is organized as follows: In Sec. II we present the variational cluster method to treat correlated systems out of equilibrium. After an introductory discussion, also in connection with previous work, we present the general method in Sec. II A. We discuss the self-consistency condition in Sec. II B. In Sec. III we introduce two specific models describing a strongly correlated Hubbard chain and a strongly correlated Hubbard ladder, respectively, which are embedded between left and right uncorrelated reservoirs with different chemical potentials and on-site energies. Effectively, this results in a voltage bias which is applied to the system. Results for the steady-state current density are discussed in Sec. IV. Finally, in Sec. V we present our conclusions and outlook.

## II. METHOD

The reason for the accuracy of CPT at short times<sup>41</sup> can be understood in simple means by observing that switching on the intercluster hopping  $V$  for a certain time  $\Delta\tau$  produces a perturbation of order  $V\Delta\tau$ , which is accounted for at first order in CPT. Therefore, we expect the result to be accurate for small  $\Delta\tau$ . At first glance, this would seem to imply that CPT is not appropriate to deal with the steady state where  $\Delta\tau \rightarrow \infty$ .

We suggest here that nonequilibrium CPT can be systematically improved by minimizing in some suitable way the “difference” between the initial state at  $\tau < \tau_0$  and the final (steady) state at  $\Delta\tau \rightarrow \infty$ . The strategy presented here to achieve this goal is to modify the parameters of the initial Hamiltonian at  $\tau < \tau_0$  in order to adapt the initial state. Since we want the long-time Hamiltonian to remain unchanged, the parameter modification is switched off at  $\tau > \tau_0$  together with switching on the intercluster hopping. For an exact calculation, and in the (quite generally realistic) assumption that the steady state does not depend on the details of the initial state, we expect results not to depend on these parameters.<sup>43</sup> However, due to the fact that the “switching” is performed perturbatively, a difference will occur. The crucial point is that one can exploit this freedom in order to “optimize” the initial state to be as close as possible to the final one.

As discussed in detail in Refs. 44,45, in equilibrium this is an alternative way to motivate the introduction of variational parameters in the variational cluster approach (VCA). The idea discussed here, thus, provides the natural extension of VCA to treat a nonequilibrium steady state. There remains to define a criterion for the

“difference” between initial and final state. (Cluster) Dynamical Mean-Field Theory<sup>46–48</sup> (DMFT) provides a natural solution, requiring the cluster-projected Green’s functions of the initial and final state to coincide. Of course, this self-consistency condition requires an infinite number of variational parameters, as well as the solution of a (cluster) impurity problem, which is computationally very expensive and whose accuracy is limited, especially in real time. In equilibrium, the selfenergy functional approach<sup>49,50</sup> (SFA) provides one possible generalization of DMFT if one wants to restrict to a finite number of variational parameters. In this case, the “difference” requirement is provided by the Euler equation (see, e.g., Eq. (7) in Ref. 49).

In the present paper, we explore an alternative criterion, whereby we require that, for a given set of variational parameters  $\mathbf{p}$ , their conjugate operators (i.e.  $dH/d\mathbf{p}$ ) have the same expectation value in the initial and in the final state. More specifically, this amounts to the condition (13). This criterion is numerically easier to implement than the SFA, since in this case it is not necessary to search for a saddle point, which is well known to be numerically expensive.<sup>51</sup> In addition, by including bath sites, self consistency conditions for dynamic correlation functions can be readily included as well, so that this criterion becomes equivalent to DMFT in the limit of an infinite number of bath sites, as SFA does.<sup>49</sup>

### A. Variational cluster approach for nonequilibrium steady state

The physical model of interest consists of a “left” and “right” noninteracting lead, as well as a central interacting region described by the Hamiltonians  $\bar{h}_L$ ,  $\bar{h}_R$ , and  $\bar{h}_C$ , respectively, see Fig. 1.  $\bar{h}_C$  contains local (Hubbard-type) interactions, as well as arbitrary single-particle terms. For  $\tau < \tau_0$ , the three regions are in equilibrium with three reservoirs at different chemical potentials,  $\mu_L$ ,  $\mu_R$ , and  $\mu_C$  respectively.<sup>52</sup> The central region is much smaller in size than the leads, so that the latter act as relaxation baths. At  $\tau = \tau_0$ , the single particle (i.e., hopping) Hamiltonian terms  $\hat{V}_{LC}$  and  $\hat{V}_{RC}$  are switched on. These connect the left and right reservoir, respectively, with the central region. The total time-dependent Hamiltonian is, thus, given by

$$H(\tau) = h + \theta(\tau - \tau_0)\hat{T}, \quad (1)$$

where  $h = \bar{h}_C + \bar{h}_L + \bar{h}_R$ , and  $\hat{T} = \hat{V}_{LC} + \hat{V}_{RC}$ . We consider here the fermionic case, although many concepts can be easily extended to bosons. The operator part  $\hat{T}$  of the time-dependent perturbation has the form

$$\hat{T} = \sum_{\mathbf{r}, \mathbf{r}'} T_{\mathbf{r}, \mathbf{r}'} c_{\mathbf{r}}^\dagger c_{\mathbf{r}'} , \quad (2)$$

where  $\mathbf{r}$  and  $\mathbf{r}'$  denote, in general, single-particle orbitals (which we term “lattice sites”), and  $c_{\mathbf{r}}$ ,  $c_{\mathbf{r}}^\dagger$  are the corresponding annihilation and creation operators. After

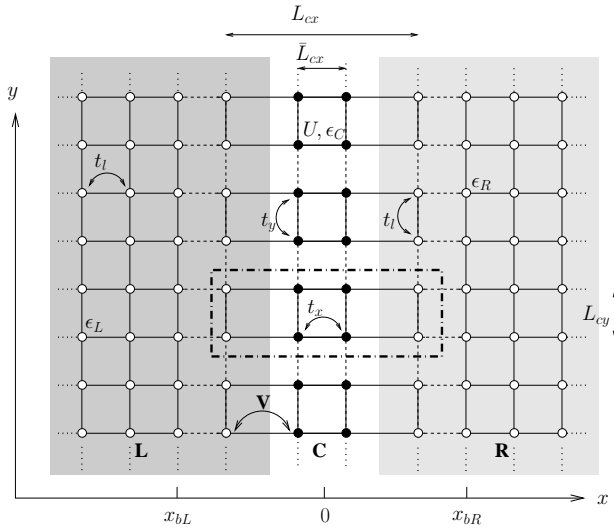


FIG. 1: Generic scheme of the physical system studied here: full (empty) circles indicate correlated (uncorrelated) lattice sites. Correlated sites are present in the physical central region (C), and are characterized by an on-site Hubbard interaction  $U$ , an on-site energy  $\epsilon_C = -U/2$ , and by hopping elements  $t_x$  and  $t_y$  in the  $x$  and  $y$  direction, respectively. The physical leads (L,R), indicated by the two shaded areas, consist of half-infinite planes described by uncorrelated tight-binding models with hopping  $t_L$ , on-site energies  $\epsilon_L$  and  $\epsilon_R$ , and chemical potentials  $\mu_L$  and  $\mu_R$ , respectively. The central region is connected to the leads via a hopping  $V$ . The width (number of sites in the  $x$  direction) of the physical central region is  $\bar{L}_{cx}$ . The height of the whole system in the  $y$  direction is infinite. In this work, we study two cases, a strongly correlated chain ( $\bar{L}_{cx} = 1$ ) and a strongly correlated two-leg ladder ( $\bar{L}_{cx} = 2$ ), both perpendicular to the applied bias. In the variational cluster calculation the central “reference” region (described by  $h_C$ ) differs from the physical one (described by  $\bar{h}_C$ ). While the latter is of the white area in the figure, the former consists of disconnected clusters aligned along the  $y$  direction, one of them being represented by the dash-dotted rectangle in the figure. The corresponding equilibrium Green’s function is determined by Lanczos exact diagonalization. The size of these clusters is  $L_c = L_{cx} \times L_{cy}$  ( $4 \times 2$  in the example). The coordinates of the boundary sites of the left (right) lead are indicated by  $x_{bL}$  ( $x_{bR}$ ). Accordingly, dashed lines represent hopping processes, which are omitted in the Hamiltonian  $h$  (for  $\tau < \tau_0$ ) and are re-included perturbatively via CPT in  $\hat{T}$ . Full lines indicate hopping terms present in  $h$ , which are thus treated exactly (see text).

a time  $\Delta\tau$  long enough for relaxation to take place, the system reaches a nonequilibrium steady state, with a particle current flowing from left to right for  $\mu_L > \mu_R$  and from right to left for  $\mu_L < \mu_R$ .

Nonequilibrium properties, in general, and nonlinear transport in particular can quite generally be determined in the frame of the Keldysh Green’s function approach.<sup>16,21,53–55</sup> Here, we adopt the notation of Ref. 16, for which the  $2 \times 2$  Keldysh Green’s function matrix is

expressed as

$$G(\mathbf{r}, \mathbf{r}' | \tau, \tau') = \begin{pmatrix} G^R & G^K \\ 0 & G^A \end{pmatrix}, \quad (3)$$

where the retarded ( $G^R$ ), advanced ( $G^A$ ), and Keldysh ( $G^K$ ) Green’s functions depend in general on two lattice sites ( $\mathbf{r}, \mathbf{r}'$ ) and two times ( $\tau, \tau'$ ). We use uppercase letters  $G$  to denote Green’s functions of the full Hamiltonian  $H(\tau)$ , and lowercase  $g$  for the ones of the decoupled Hamiltonian  $h$ . Of course, at  $\tau < \tau_0$ ,  $g = G$ . Both for  $\tau < \tau_0$  as well as in steady state, time translation invariance holds, so that Green’s functions depend only on the time difference  $\tau - \tau'$ , and we can Fourier transform to frequency space  $\omega$ .

Generally, there are the following two situations: (i) The central region is small enough so that its equilibrium Green’s function (say, the retarded one  $g_{CC}^R(\omega)$ ) can be evaluated exactly by Lanczos diagonalization or by quantum Monte-Carlo simulations.<sup>56</sup> The Keldysh Green’s function is then given by<sup>21</sup>  $g_{CC}^K(\omega) = (g_{CC}^R(\omega) - g_{CC}^A(\omega)) s_C(\omega)$ , where  $s_C(\omega) \equiv (2 - f_F(\omega - \mu_C))$ , and  $f_F$  is the Fermi function. (ii) When the central region is large, as it is the case for the model we will consider here, it can be itself split into clusters which are small enough to be solved exactly. Let  $h_{ic}$  be the intercluster Hamiltonian of the central region. We can formally include  $h_{ic}$  into the “perturbation” part  $\hat{T}$ , i. e.,  $\hat{T} = \hat{V}_{LC} + \hat{V}_{RC} + h_{ic}$ , and subtract it from  $h$ , i. e.,  $h = h_C + \bar{h}_L + \bar{h}_R$ , with  $h_C = \bar{h}_C - h_{ic}$ . In this way, we modify the Hamiltonian for  $\tau < \tau_0$ , but the total Hamiltonian at  $\tau > \tau_0$  remains unchanged. Also in this case, the Green’s function  $g_{CC}$  associated with the Hamiltonian  $h_C$  can be solved exactly. Under the assumption that the steady state is unique and thus only depends on the final Hamiltonian  $H(\tau \rightarrow \infty)$ , results for the steady state should, in principle, not depend on this transformation, provided the time-dependence was solved exactly. This is, for example, easy to verify in the noninteracting case.

The equilibrium Green’s functions  $g_{LL}$  ( $g_{RR}$ ) of the isolated leads can be evaluated exactly (or to arbitrary precision), as their Hamiltonians are noninteracting ones. Moreover, for the treatment of the nonequilibrium problem only values of  $g_{LL}$  ( $g_{RR}$ ) in a small number of  $\mathbf{r}$  points enter the Dyson equation, see (9), below, and also Ref. 21. As above, the Keldysh Green’s function of the left lead is given in frequency space by

$$g_{LL}^K = -2i \pi \rho_{LL}(\omega) s_L(\omega) \quad (4)$$

with  $s_L(\omega) = (2 - f_F(\omega - \mu_L))$  and  $-2i \pi \rho_{LL}(\omega) = (g_{LL}^R - g_{LL}^A)$  is the density of states. A similar result is obtained for the right lead.

A short remark should be made about initial correlations, which, in principle, should have to be accounted for by a path in the “Matsubara” direction.<sup>57</sup> However, here we are considering the steady state, which we expect not to be affected by the Matsubara part of the contour as

opposed to the short time dynamics.<sup>16,21</sup> In addition, it was shown in Ref. 41 that these vanish in CPT, provided one starts from an equilibrium state of the cluster.

The advantage of using the Keldysh Green's function matrix representation is that one can express Dyson's equation in the same form as in equilibrium.<sup>16,21</sup> In our case, we can write it in the form

$$G = g + g (T + \Delta\Sigma) G, \quad (5)$$

where  $g = \text{diag}(g_{CC}, g_{LL}, g_{RR})$  is block diagonal, and the products have to be considered as matrix multiplications.<sup>58</sup> In (5),  $\Delta\Sigma = \Sigma - \Sigma_C$  is the difference between the total self-energy  $\Sigma$  of the coupled cluster+leads system and the self-energy  $\Sigma_C$  associated with  $h$ . Both self-energies are nonzero on the central region only, since the leads are noninteracting.

The CPT approximation<sup>59</sup> precisely amounts to neglecting  $\Delta\Sigma$ . As pointed out in Ref. 41 this corresponds to neglecting irreducible diagrams containing interactions and one or more  $T$  terms. In this approximation, (5) can be used to obtain an equation for the Green's function  $G_{CC}$  projected onto the central region, which is still a matrix in the lattice sites of the central region and in Keldysh space<sup>60</sup>

$$\begin{aligned} G_{CC} &= g_{CC} + g_{CC} T_{CC} G_{CC} + \\ &+ g_{CC} T_{CL} G_{LC} + g_{CC} T_{CR} G_{RC}, \end{aligned} \quad (6)$$

and for the lead-central region Green's functions:

$$\begin{aligned} G_{LC} &= g_{LL} T_{LC} G_{CC} \\ G_{RC} &= g_{RR} T_{RC} G_{CC}. \end{aligned} \quad (7)$$

Insertion of (6) into (7) yields

$$G_{CC} = g_{CC} + g_{CC} \Sigma_{CC}^{\text{eff}} G_{CC} \quad (8)$$

with the effective self-energy

$$\Sigma_{CC}^{\text{eff}} = T_{CC} + T_{CL} g_{LL} T_{LC} + T_{CR} g_{RR} T_{RC}. \quad (9)$$

One finally obtains a solution in the usual form<sup>61</sup>

$$G_{CC} = g_{CC} (1 - \Sigma_{CC}^{\text{eff}} g_{CC})^{-1}. \quad (10)$$

For the evaluation of the current from, say, the left lead to the central region one needs the  $G_{LC}$  Green's function, which is readily obtained by combining (7) with (10).

For the numerical implementation it is convenient to exploit the fact that all two-point matrices  $m$  in site and Keldysh space can be expressed in block form as

$$m = \begin{pmatrix} m^R & m^K \\ 0 & m^A \end{pmatrix}. \quad (11)$$

Inversions of these matrices can be expressed as

$$m^{-1} = \begin{pmatrix} (m^R)^{-1} & -(m^R)^{-1} m^K (m^A)^{-1} \\ 0 & (m^A)^{-1} \end{pmatrix}. \quad (12)$$

In the end, one needs to invert matrices with a dimension at most as large as the number of sites in the central region. In the case investigated here, the central region is translation invariant in  $y$ -direction and can be split up into identical clusters. Thus, one can apply an appropriate Fourier transform and restrict to the inversion of matrices with a dimension equal to the number of cluster sites ( $L_{cx} \times L_{cy}$ ).

## B. Self-consistency condition

Equation (10) is the expression for the Green's function of the central region in the CPT approximation. As discussed above, one would like to optimize the initial state by suitably adjusting the parameters of the “initial” ( $\tau < \tau_0$ ) Hamiltonian. Besides splitting the central region into clusters, we have the additional freedom to subtract from the intercluster Hamiltonian  $h_{ic}$  an arbitrary intracenter single-particle Hamiltonian  $\Delta h$ , i. e.,  $h_{ic} \rightarrow h_{ic} - \Delta h$ . This term must then be added to the initial Hamiltonian  $h$ , so that the final  $\tau > \tau_0$  total Hamiltonian is independent of  $\Delta h$ . While exact results should not depend on  $\Delta h$  (this can be, for example, verified in the noninteracting case), physical quantities will in fact depend on  $\Delta h$ , due to the approximate treatment of the perturbation  $\hat{T}$  which includes  $-\Delta h$  (see a similar discussion on this issue in Refs. 44,45). This freedom, however, can be exploited in order to optimize the final result. In the present paper the variational condition amounts to requiring that the expectation values of operators coupled to the variational parameters  $\mathbf{p}$  contained in  $\Delta h$  be equal at  $\tau < \tau_0$  and in steady state. More specifically, we impose the condition<sup>62</sup>

$$\int \frac{d\omega}{2\pi} \text{tr} (g_{CC}^K - G_{CC}^K) \frac{\partial (g_{0CC}^R)^{-1}}{\partial \mathbf{p}} = 0, \quad (13)$$

where  $g_{0CC}^R$  is the noninteracting retarded Green's function associated with  $h_C$ . In this way one attempts to “optimize” the difference between initial and final state and to “minimize” the effect of the perturbation.

A second systematic improvement consists in increasing the cluster size  $L_c$ . This can be done in two ways: (i) by extending the boundaries of the central region in  $y$  direction and thus treating more correlated sites exactly and (ii) by extending the boundaries in  $x$  direction to include an increasing number of uncorrelated lattice sites, i. e., taking  $L_{cx} > \bar{L}_{cx}$ , cf. Fig. 1. Again, results at large times are expected not to depend on the exact position of the boundaries. Importantly, within the present approximation, considering more sites amounts to taking into account to some degree the  $V$ -induced renormalization of the self-energy.

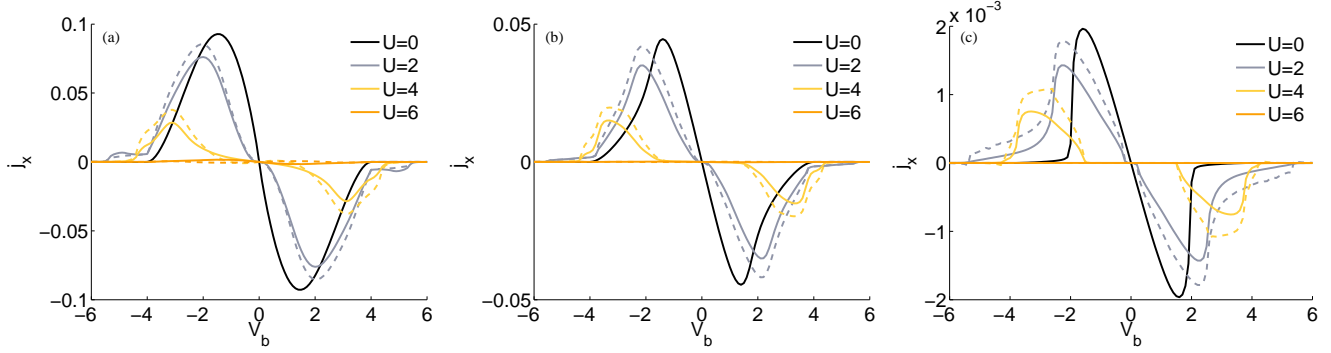


FIG. 2: (Color online) Steady-state current density  $j_x$  (in units of  $t_l = 1$ ,  $a = 1$ ,  $\hbar = 1$ , and  $e = 1$ ) as a function of bias voltage  $V_b \equiv \mu_R - \mu_L$  of a correlated two-leg ladder ( $\bar{L}_{cx} = 2$ ). The steady-state current density is evaluated for different values of the lead to central region hopping (a)  $V = 1.0$ , (b)  $V = 0.5$ , and (c)  $V = 0.1$ , and of the interaction  $U$ , see legend. Results are obtained with clusters of size  $L_c = L_{cx} \times L_{cy} = 2 \times 2$ . Solid lines are results obtained with (15), whereas dashed lines are obtained by using  $G_{CC}^K$  instead of  $G_{LC}^K$  (see text).

### III. MODEL

Next, we present an application of the nonequilibrium VCA method described in Sec. II. Specifically, we study nonlinear transport properties across an extended correlated region (C in Fig. 1), which we take to be a Hubbard chain ( $\bar{L}_{cx} = 1$ ) or a Hubbard ladder ( $\bar{L}_{cx} = 2$ ) with nearest-neighbor hoppings  $t_x$  and  $t_y$ , on-site interaction  $U$ , on-site energy  $\epsilon_C$ , and chemical potential  $\mu_C$ . The leads (shaded regions in Fig. 1) are described by two-dimensional semiinfinite tight-binding models with nearest-neighbor hopping  $t_l$ , on-site energies  $\epsilon_L$  and  $\epsilon_R$ , and chemical potential  $\mu_L$  and  $\mu_R$  for the left and right lead, respectively. We apply a bias voltage  $V_b$  to the leads by setting  $\mu_R = \epsilon_R = V_b/2$  and restrict to the particle-hole symmetric case where  $\epsilon_C = -U/2$ ,  $\mu_C = 0$ ,  $\epsilon_R = -\epsilon_L$ , and  $\mu_L = -\mu_R$ . For simplicity, we neglect the long-range part of the Coulomb interaction. Under some conditions, this can be absorbed within the single-particle parameters of the Hamiltonian, in a mean-field sense<sup>21</sup>.

As discussed above, the  $\tau < \tau_0$  Hamiltonian  $h$  does not necessarily coincide with the physical partition into leads and central region.  $h$  is obtained by tiling the total system into small clusters as illustrated in Fig. 1, as well as by adding an intracluster variational term  $\Delta h$ . In the present case, we take  $\Delta h$  to contain a correction  $\Delta t_x$  to the interladder hopping. Further options could include, for example, a site-dependent change in the on-site energy  $\Delta\epsilon_C(x)$ . Particle-hole symmetry can be preserved by constraining this change to be antisymmetric:  $\Delta\epsilon_C(x) = -\Delta\epsilon_C(-x)$ . In this paper, whose goal is to carry out a first test of the method, we restrict, for simplicity, to a single variational parameter. The choice of  $\Delta t_x$  as a variational parameter is motivated by the fact that this term is important for the current flowing in  $x$ -direction. According to the prescription discussed above, we require the expectation value of the real part of the

kinetic energy in  $x$  direction evaluated with  $g_{CC}$  and with  $C_{CC}$  to coincide.

One comment about the chemical potential. In principle when including some of the sites of the leads in  $h$ , i.e., when  $L_{cx} > \bar{L}_{cx}$ , then these additional sites have a chemical potential  $\mu_C$  which differs from the one they would have if  $L_{cx} = \bar{L}_{cx}$  (i.e.,  $\mu_L$  or  $\mu_R$ ). However, the initial state, i.e., chemical potential, of these sites does not affect the steady state, as their volume-to-surface ratio is finite. Of course, their on-site energies ( $\epsilon_R$  and  $\epsilon_L$ ) are important, and should not be modified (unless it is treated as a variational parameter).

Due to translation invariance by a cluster length  $L_{cy}$  in the  $y$ -direction, it is convenient, as in usual VCA, to carry out a Fourier transformation in  $y$  direction, with associated momenta  $q_y$ . The Green's functions  $g_{CC}$  and  $G_{CC}$ , as well as  $T$  become now functions of two momenta  $q_y + Q_y$  and  $q_y + Q'_y$ , where  $Q_y$  and  $Q'_y$  are reciprocal superlattice vectors of which there are only  $L_{cy}$  inequivalent ones. The Green's functions of the leads at the boundary sites to the central region must be expressed in the same basis. This can be evaluated analytically for a semiinfinite tight-binding model in the following way. Let  $g_{LL}(x_{bL}|y - y'|z)$  be the Green's function of the boundary site of the left lead at complex frequency  $z$ , then

$$g_{LL}(x_{bL}|q_y|z) = \sum_y e^{-iq_y y} g_{LL}(x_{bL}|y - 0|z)$$

is the associated Fourier transform in the  $y$  direction. Due to translation invariance, this is diagonal in the  $q_y$  basis. The latter can be easily shown to be related to the Green's function  $g_{hc}(1, 1|z)$  of the end-point of a tight-binding chain with open boundary conditions and with zero on-site energy by

$$g_{LL}(x_{bL}|q_y|z) = g_{hc}(1, 1|z - 2t_l \cos q_y - \epsilon_L). \quad (14)$$

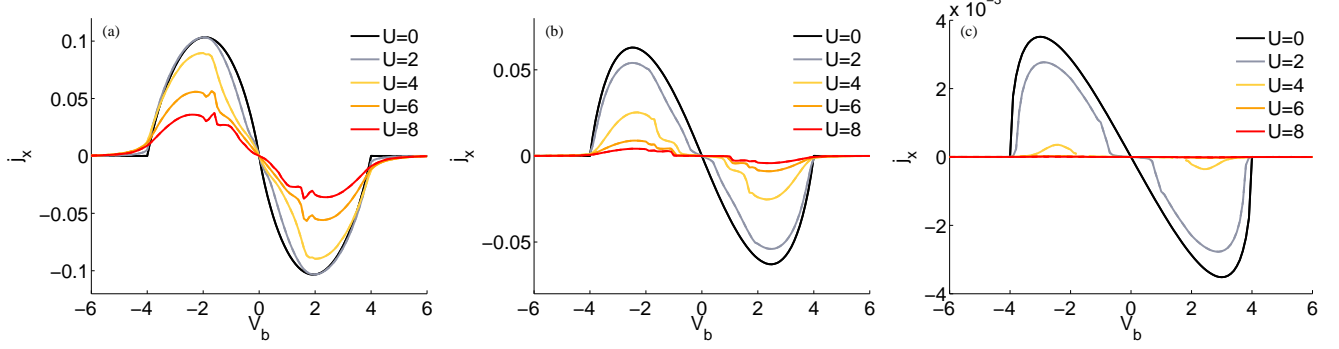


FIG. 3: (Color online) Steady-state current density  $j_x$  as in Fig. 2 but for the correlated chain ( $\bar{L}_{cx} = 1$ ). The current density is evaluated for different values of the lead to central region hopping (a)  $V = 1.0$ , (b)  $V = 0.5$ , and (c)  $V = 0.1$ , and of the interaction  $U$ , see legend. Results are obtained for clusters of size  $L_c = L_{cx} \times L_{cy} = 3 \times 2$ .

The analytic form of  $g_{hc}(x, x'|z)$  can be easily evaluated

$$g_{hc}(x, x'|z) = g_{tb}(x + x'|z) - g_{tb}(x - x'|z),$$

where  $g_{tb}(x - x'|z)$  is the tight-binding Green's functions of the infinite chain with periodic boundary conditions.<sup>63</sup>

The retarded (advanced) Green's functions are obtained as usually, by setting  $z \rightarrow \omega + i0^+$  ( $z \rightarrow \omega - i0^+$ ). Notice that the retarded and advanced Green's functions are evaluated without chemical potential. The latter enters the expression for the Keldysh Green's function (4) only.

#### IV. RESULTS

We have evaluated the steady-state current density  $j_x$  of the models discussed in Sec. III as a function of the bias  $V_b \equiv \mu_R - \mu_L = 2\mu_R$  between the leads. Simultaneously to the chemical potential the on-site energy is adjusted  $\epsilon_{L/R} = \mu_{L/R}$ . This corresponds to a total shift of the density of states. The steady-state current  $j_x$  is obtained from the lead to central region Green's function  $G_{LC}$  as

$$j_x = t(x_{bL}, x_{bL} + 1) \sum_{y, q_y} \int_{-\infty}^{\infty} \frac{d\omega}{2\pi} \text{Re} G_{LC}^K(\mathbf{r}, \mathbf{r}' | q_y | \omega) \quad (15)$$

with  $\mathbf{r} = (x_{bL}, y)$ ,  $\mathbf{r}' = (x_{bL} + 1, y)$ , and  $t(x_{bL}, x_{bL} + 1)$  is the hopping between these adjacent sites (i.e.,  $t_l$  or  $V$ ).<sup>64</sup> For  $L_{cy} \geq 2$ , the current can be alternatively evaluated from  $G_{CC}^K$  by considering two adjacent lattice sites along the  $x$  direction in the central region.

In Fig. 2 we display the steady-state current density  $j_x$  of the two-leg ladder ( $\bar{L}_{cx} = 2$ ), as a function of the bias voltage  $V_b$  for different values of the interaction strength  $U = \{0, 2, 4, 6\}$  and lead-to-system couplings (a)  $V = 1.0$ , (b)  $V = 0.5$ , and (c)  $V = 0.1$ . We use  $\hbar = 1$  and  $t_l = 1$  which sets the unity of energy and the inverse unit of time. Moreover, we take the lattice constant  $a = 1$ . The hopping is uniform in the whole

system, meaning that  $t_x, t_y$  in the central region and  $t_l$  of the leads are equal. The on-site energy of the central region is  $\epsilon_c = -U/2$  corresponding to half-filling, whereas the on-site energy of the left (right) lead is equal to its chemical potential  $\mu_L$  ( $\mu_R$ ). The central region is decomposed into clusters of size  $L_c = 2 \times 2$ . In all panels (a)–(c), we plot the current density between the left lead and the central region (solid lines) and between two adjacent lattice sites of the central region (dashed lines). The current density is evaluated with Eq. (15), where the appropriate Keldysh Green's functions  $G_{LC}$  and  $G_{CC}$ , respectively, are inserted. There is a slight discrepancy between the two results. This could be due to the fact that the method is not completely conserving and, thus, the continuity equation is not completely fulfilled. However, from our results we see that the deviation from the continuity equation is quite small, see Fig. 2.

All results are determined self-consistently using  $\Delta t_x$  as variational parameter, see Sec. III, by requiring that the correlator  $\text{Re} \langle c_{x,y}^\dagger c_{x+1,y} \rangle_h$  at  $\tau < \tau_0$  is identical to the correlator  $\text{Re} \langle c_{x,y}^\dagger c_{x+1,y} \rangle_{H(\tau \rightarrow \infty)}$  in steady state, where  $x$  belongs to the central region  $C$ .

For increasing bias voltage  $V_b$  the modulus of the steady-state current density  $j_x$  initially increases. At a certain value of  $V_b$  it reaches a maximum. When increasing the bias the current density drops again, as the overlap between the density of states of the central region and the leads decreases. Importantly, the current is strongly suppressed in the gapped region of the two-leg ladder, i.e. for small bias voltage  $V_b$ . This is particularly visible for small coupling  $V$  to the leads, since the  $\delta$ -peaks, composing the initial density of states of the central region are broadened by the coupling to the leads. Note the different scales in (a)–(c). Specifically, the maximum of the current is reduced by roughly a factor 50, when decreasing the coupling between the leads and the central region by a factor 10. In addition the current is suppressed with increasing interaction  $U$ . For  $U = 4$  the maximum is roughly reduced by a factor of two as compared to the noninteracting case, whereas for  $U = 6$  the

current is already almost zero for arbitrary voltage bias  $V_b$ .

In Fig. 3 we show the steady-state current density  $j_x$  of the correlated chain ( $\bar{L}_{cx} = 1$ ) as a function of the bias voltage. The parameters are the same as in the case of the two-leg ladder, however, the central region is decomposed into clusters of size  $L_c = 3 \times 2$ , where also sites of the leads are taken into account to improve the results. The half-filled Hubbard chain is gapped as well. As for the two-leg ladder the gap behavior in the current is more pronounced for smaller lead to central region coupling  $V = 0.1$ . In contrast, for strong coupling  $V = 1.0$ , (a), the current does not show any gap behavior due to the strong hybridization with the leads. However, with decreasing coupling, (b)–(c), the current is strongly suppressed for large interaction  $U$ . Importantly, for the correlated chain the continuity equation is strictly fulfilled. There is no deviation in the steady-state current density  $j_x$  evaluated between the lead and the central region and between two adjacent sites within the central region. This is probably due to the absence of vertex corrections at the uncorrelated sites.

Next, we study the convergence with the size of the reference cluster, as well as the effect of the self-consistency condition. The results for the two-leg ladder are depicted in Fig. 4. Results in (a) are obtained by optimizing  $\Delta t_x$  as variational parameter as described in Sec. III, whereas (b) shows results without variational parameters, i. e. of steady-state CPT. It can be observed, that the variational parameters significantly improve the results, as the convergence for  $j_x$  is much more rapid with increasing cluster size as compared to the case without self-consistency.

Now we turn to the case of the correlated chain. The corresponding current densities are shown in Fig. 5 for different cluster sizes. Results for  $L_c = 1 \times 2$  and  $L_c = 1 \times 4$  are obtained without variational principle, as the cluster does not contain a hopping in  $x$  direction, whereas results for  $L_c = 3 \times 1$  and  $L_c = 3 \times 2$  are obtained by optimizing  $\Delta t_x$ . The results for the strongly correlated chain show that it seems to be important to include some noncorrelated lead sites in the cluster of the central region, since only then signatures of the gap emerge in the steady state current density.

The figures show that there are cluster geometries that, even with self-consistency, provide results far from convergence. This is the case for clusters with  $L_{cy} = 1$ . For the chain this is probably due to the degeneracy of the cluster ground state. For the ladder, it seems that using as starting point the  $2 \times 1$  dimer exaggerates the gap. But besides these data obtained from admittedly very small clusters, results converge quickly as a function of cluster sizes provided the hopping in  $x$  direction is used as a variational parameter.

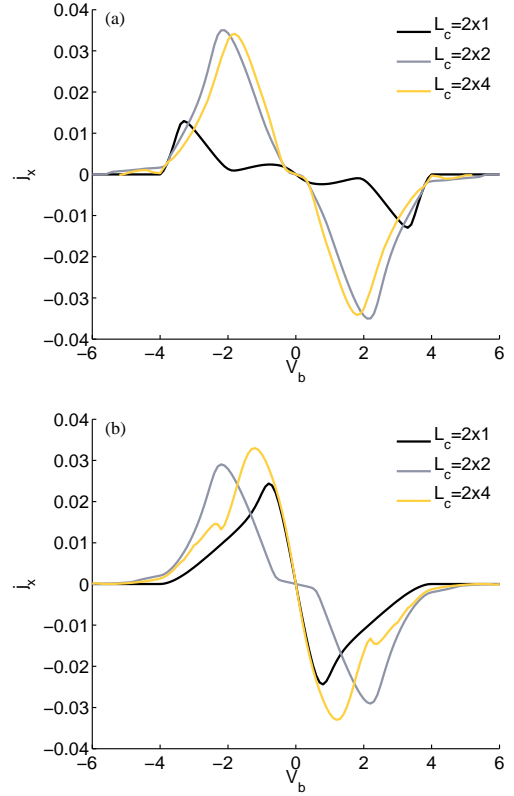


FIG. 4: (Color online) Convergence of the steady-state current density  $j_x$  with cluster size  $L_c = L_{cx} \times L_{cy}$  for the correlated two-leg ladder. Results in (a) are obtained with variational principle and (b) without variational principle. The parameters are the same as in Fig. 2 except that  $U = 2$  and  $V = 0.5$ .

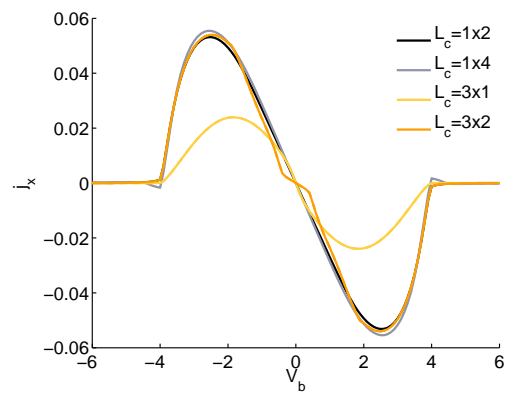


FIG. 5: (Color online) Convergence of the steady-state current density  $j_x$  with cluster size  $L_c = L_{cx} \times L_{cy}$  for the correlated chain. Results for  $L_c = 1 \times 2$  or  $L_c = 1 \times 4$  are obtained without variational principle, whereas results for  $L_c = 3 \times 1$  or  $L_c = 3 \times 2$  are obtained with variational principle. The parameters are the same as in Fig. 4.

## V. CONCLUSIONS

In this paper we have presented a novel variational cluster approach to treat strongly correlated systems in the nonequilibrium steady state. The idea is based on a variational cluster method extended to the Keldysh formalism,<sup>41</sup> which, for the steady state, becomes translation invariant in time and thus can be worked out in frequency space.

The variational extension is similar in spirit to the equilibrium case, in which one “adds” single-particle terms to the cluster Hamiltonian which is then solved exactly, and “subtract” them perturbatively.<sup>44,45</sup> The values of the parameters are determined by some requirement which in the end amounts to optimize the unperturbed state with respect to the perturbed one. We have presented results for the current across a correlated extended region (a Hubbard chain or ladder) in contact with two uncorrelated reservoirs at different chemical potentials. The advantage of the method is that one can work with truly infinite leads and at truly large times. Both are necessary conditions in order to reach the steady state.

There is a certain freedom in choosing the most appropriate variational criterion. Here we have required the operators associated with the variational parameters to have the same expectation values in the unperturbed and in perturbed state. Certainly, an interesting alternative would be to generalize the variational criterion provided by the SFA<sup>49</sup> to the nonequilibrium case. While it is not clear what would be the appropriate generalization of the grand-potential in the nonequilibrium case, one should expect that the Euler equation (Eq. (7) of Ref. 49), suitably generalized to the Keldysh contour, can be readily extended to the nonequilibrium case. In any case, both methods, SFA and the present one, become equivalent to (cluster)-DMFT in the case in which an infinite number of variational parameters is suitably taken. In general, we expect results to improve when more variational parameters are taken into account. In

particular, when evaluating the current across the central region, it would be useful if a current was already flowing in the cluster. This can be achieved by adding a complex variational hopping between the end points of the cluster, and of course remove it perturbatively. The corresponding variational condition would contain the interesting requirement that the current flow in this modified cluster be the same as in steady state.

The generalization to the case in which the leads are interacting is in principle straightforward. However, a certain translation invariance should be preserved in order for the calculation to remain feasible within a reasonable computational effort.

The model studied here, is motivated by the interest in transport across semiconductor heterostructures (see, e.g. 10,11,65,66). However, it is well known that in this case charging effects are important, also near the boundaries between the leads and the central region. Here, scattering effects produce charge density waves, which, when taking into account the long-range part of the Coulomb interaction, even in mean-field, produce a modification of the single-particle potential. In order to treat realistic structures, these effects should be included at the Hartree-fock level at least. All these generalizations can be straightforwardly treated with the presented variational cluster method, however, in this work we focus on a first proof of concept study and application containing the essential ingredients for the investigation of the nonequilibrium steady state of strongly correlated many-body systems.

## Acknowledgments

We acknowledge fruitful discussions with S. Diehl. We made use of the ALPS library.<sup>67</sup> Financial support from the Austrian Science Fund (FWF) under Projects No. P18551-N16, and P21289-N16 are gratefully acknowledged.

\* michael.knap@tugraz.at

<sup>1</sup> D. Jaksch, C. Bruder, J. I. Cirac, C. W. Gardiner, and P. Zoller, Phys. Rev. Lett. **81**, 3108 (1998).

<sup>2</sup> M. Greiner, O. Mandel, T. Esslinger, T. W. Hänsch, and I. Bloch, Nature (London) **415**, 39 (2002).

<sup>3</sup> I. Bloch, J. Dalibard, and W. Zwerger, Rev. Mod. Phys. **80**, 885 (2008).

<sup>4</sup> M. Hartmann, F. G. Brandão, and M. B. Plenio, Laser & Photonics Rev. **2**, 527 (2008).

<sup>5</sup> A. Tomadin and R. Fazio, J. Opt. Soc. Am. B **27**, A130 (2010).

<sup>6</sup> H. Park, J. Park, A. K. L. Lim, E. H. Anderson, A. P. Alivisatos, and P. L. McEuen, Nature **407**, 57 (2000).

<sup>7</sup> J. Paaske and K. Flensberg, Phys. Rev. Lett. **94**, 176801 (2005).

<sup>8</sup> L. L. Bonilla and H. T. Grahn, Rep. Prog. Phys. **68**, 577 (2005).

<sup>9</sup> T. Jungwirth, J. Sinova, J. Masek, J. Kucera, and A. H. MacDonald, Rev. Mod. Phys. **78**, 809 (2006).

<sup>10</sup> C. Ertler, W. Pötz, and J. Fabian, Appl. Phys. Lett. **97**, 042104 (2010).

<sup>11</sup> C. Ertler, P. Senekowitsch, J. Fabian, and W. Pötz, in *Computational Electronics (IWCE), 2010 14th International Workshop on* (2010), pp. 1–4.

<sup>12</sup> I. Zutic, J. Fabian, and S. D. Sarma, Rev. Mod. Phys. **76**, 323 (2004).

<sup>13</sup> J. Fabian, A. Matos-Abiague, C. Ertler, P. Stano, and I. Zutic, Acta Physica Slovaca **57**, 565 (2007).

<sup>14</sup> A. Slobodskyy, C. Gould, T. Slobodskyy, C. R. Becker, G. Schmidt, and L. W. Molenkamp, Phys. Rev. Lett. **90**,

246601 (2003).

<sup>15</sup> K. Sokolowski-Tinten, C. Blome, J. Blums, A. Cavalieri, C. Dietrich, A. Tarasevitch, I. Uschmann, E. Forster, M. Kammler, M. Horn-von Hoegen, et al., *Nature* **422**, 287 (2003).

<sup>16</sup> J. Rammer and H. Smith, *Rev. Mod. Phys.* **58**, 323 (1986).

<sup>17</sup> Y. Meir and N. S. Wingreen, *Phys. Rev. Lett.* **68**, 2512 (1992).

<sup>18</sup> Y. Meir, N. S. Wingreen, and P. A. Lee, *Phys. Rev. Lett.* **70**, 2601 (1993).

<sup>19</sup> Schoeller, H., *Eur. Phys. J. Special Topics* **168**, 179 (2009).

<sup>20</sup> D. A. Ryndyk, R. Gutierrez, B. Song, and G. Cuniberti (2008), arXiv:0805.0628.

<sup>21</sup> H. Haug and A.-P. Jauho, *Quantum Kinetics in Transport and Optics of Semiconductors* (Springer, Heidelberg, 1998).

<sup>22</sup> B. Kraus, H. P. Büchler, S. Diehl, A. Kantian, A. Micheli, and P. Zoller, *Phys. Rev. A* **78**, 042307 (2008).

<sup>23</sup> S. Diehl, A. Micheli, A. Kantian, B. Kraus, H. P. Büchler, and P. Zoller, *Nat. Phys.* **4**, 878 (2008).

<sup>24</sup> S. Diehl, A. Tomadin, A. Micheli, R. Fazio, and P. Zoller, *Phys. Rev. Lett.* **105**, 015702 (2010).

<sup>25</sup> H. Pichler, A. J. Daley, and P. Zoller, *Phys. Rev. A* **82**, 063605 (2010).

<sup>26</sup> A. Tomadin, S. Diehl, and P. Zoller, *Phys. Rev. A* **83**, 013611 (2011).

<sup>27</sup> P. Barmettler and C. Kollath, arXiv:1012.0422 (2010).

<sup>28</sup> S. R. White and A. E. Feiguin, *Phys. Rev. Lett.* **93**, 076401 (2004).

<sup>29</sup> A. J. Daley, C. Kollath, U. Schollwöck, and G. Vidal, *J. Stat. Mech.* **2004**, P04005 (2004).

<sup>30</sup> T. Prosen and M. Znidaric, *Journal of Statistical Mechanics: Theory and Experiment* **2009**, P02035 (2009).

<sup>31</sup> G. Benenti, G. Casati, T. Prosen, D. Rossini, and M. Žnidarič, *Phys. Rev. B* **80**, 035110 (2009).

<sup>32</sup> D. Perez-Garcia, F. Verstraete, M. M. Wolf, and J. I. Cirac, *Quant. Inf. Comp.* **7**, 401 (2007).

<sup>33</sup> P. Werner, T. Oka, and A. J. Millis, *Phys. Rev. B* **79**, 035320 (2009).

<sup>34</sup> S. G. Jakobs, V. Meden, and H. Schoeller, *Phys. Rev. Lett.* **99**, 150603 (2007).

<sup>35</sup> F. B. Anders and A. Schiller, *Phys. Rev. Lett.* **95**, 196801 (2005).

<sup>36</sup> A. V. Joura, J. K. Freericks, and T. Pruschke, *Phys. Rev. Lett.* **101**, 196401 (2008).

<sup>37</sup> J. K. Freericks, V. M. Turkowski, and V. Zlaticacute, *Phys. Rev. Lett.* **97**, 266408 (2006).

<sup>38</sup> M. Eckstein, M. Kollar, and P. Werner, *Phys. Rev. Lett.* **103**, 056403 (2009).

<sup>39</sup> P. Mehta and N. Andrei, *Phys. Rev. Lett.* **96**, 216802 (2006).

<sup>40</sup> C. Jung, A. Lieder, S. Brener, H. Hafermann, B. Baxevanis, A. Chudnovskiy, A. N. Rubtsov, M. I. Katsnelson, and A. I. Lichtenstein, arXiv:1011.3264 (2010).

<sup>41</sup> M. Balzer and M. Potthoff (2011), arXiv:1102.3344.

<sup>42</sup> B. Doyon and N. Andrei, *Phys. Rev. B* **73**, 245326 (2006).

<sup>43</sup> Multistable systems present an interesting exception.

<sup>44</sup> M. Knap, E. Arrigoni, and W. von der Linden, *Phys. Rev. B* **83**, 134507 (2011).

<sup>45</sup> C. Dahnken, M. Aichhorn, W. Hanke, E. Arrigoni, and M. Potthoff, *Phys. Rev. B* **70**, 245110 (2004).

<sup>46</sup> W. Metzner and D. Vollhardt, *Phys. Rev. Lett.* **62**, 324 (1989).

<sup>47</sup> A. Georges, G. Kotliar, W. Krauth, and M. J. Rozenberg, *Rev. Mod. Phys.* **68**, 13 (1996).

<sup>48</sup> G. Kotliar, S. Y. Savrasov, G. Pálsson, and G. Biroli, *Phys. Rev. Lett.* **87**, 186401 (2001).

<sup>49</sup> M. Potthoff, *Eur. Phys. J. B* **32**, 429 (2003).

<sup>50</sup> M. Potthoff, *Eur. Phys. J. B* **36**, 335 (2003).

<sup>51</sup> A. H. Nevidomskyy, D. Sénéchal, and A. M. S. Tremblay, *Phys. Rev. B* **77**, 075105 (2008).

<sup>52</sup> Although, for simplicity, we are considering zero temperature  $T = 0$  here, it is straightforward to consider the case in which the regions are initially in contact with baths at different temperatures.

<sup>53</sup> L. P. Kadanoff and G. Baym, *Quantum statistical mechanics: Green's function methods in equilibrium and nonequilibrium problems* (Addison-Wesley, Redwood City, Calif., 1962).

<sup>54</sup> J. Schwinger, *J. Math. Phys.* **2**, 407 (1961).

<sup>55</sup> L. V. Keldysh, *Sov. Phys. JETP* **20**, 1018 (1965).

<sup>56</sup> Here, we consider  $g_{CC}^R$  as a matrix in the lattice indices  $\mathbf{r}, \mathbf{r}'$ , which is of course zero for  $\mathbf{r}$  or  $\mathbf{r}'$  not belonging to the central region.

<sup>57</sup> M. Wagner, *Phys. Rev. B* **44**, 6104 (1991).

<sup>58</sup> In the time representation (3) they also include convolutions over internal times. However, since we are considering the steady state, Green's functions become diagonal in the frequency representation.

<sup>59</sup> D. Sénéchal, D. Perez, and M. Pioro-Ladrière, *Phys. Rev. Lett.* **84**, 522 (2000).

<sup>60</sup> Here, we use a notation to express projection of objects such as  $G$ ,  $T$ , etc, which are matrices in lattice indices and in Keldysh space, onto one of the three regions  $m$  be such a matrix, then  $m_{AB}$  refers to a sub-matrix of  $m$  in which the left (right) index is restricted to region  $A$  ( $B$ ), with  $A, B = C, L$ , or  $R$ .

<sup>61</sup> Of course, for the given approximation, the final expression for the current is equivalent to the one obtained in Ref. 17 (see also Ref. 21). However, for the numerical implementation, we find the path pursued here more convenient.

<sup>62</sup> This expression should be compared with the SFA condition, Eq. (7) of Ref. 49.

<sup>63</sup> E. N. Economou, *Green's Functions in Quantum Physics* (Springer, Heidelberg, 2006).

<sup>64</sup> One should mention that the evaluation of integrals like (15) are quite tricky. While all  $\delta$  peaks are broadened by the peaks, especially for small  $V$ . In addition, the integral must be carried out on the real axis, as there are no causality relations which allow to distort the contour like, for example, in Ref. 68.

<sup>65</sup> S. Pérez-Merchancano, H. P. Gutiérrez, and G. E. Marques, *Microelectronics Journal* **39**, 1339 (2008), Papers CLACSA XIII, Colombia 2007.

<sup>66</sup> L. Chioncel, I. Leonov, H. Allmaier, F. Beiuseanu, E. Arrigoni, T. Jurcut, and W. Pötz, *Phys. Rev. B* **83**, 035307 (2011).

<sup>67</sup> A. Albuquerque, F. Alet, P. Corboz, P. Dayal, A. Feiguin, S. Fuchs, L. Gamper, E. Gull, S. Gürtler, A. Honecker, et al., *J. Magn. Magn. Mater.* **310**, 1187 (2007).

<sup>68</sup> X. Lu and E. Arrigoni, *Phys. Rev. B* **79**, 245109 (2009).